GRADIENT OF SHORTENING AND VERTICAL-AXIS ROTATIONS IN THE SOUTHERN PYRENEES (SPAIN), INSIGHTS FROM A SYNTHESIS OF PALEOMAGNETIC DATA

B. Oliva-Urcia [1,2] and E.L. Pueyo [3]

[1] *Structural Geology, Universidad de Zaragoza, Pedro Cerbuna 12, 50009 Zaragoza. boliva@unizar.es*
[2] *Geological Sciences, University of Michigan, USA.*
[3] *Unidad de Geología y Geofísica. Instituto Geológico y Minero de España. Spain.*

Resumen: Los cortes compensados y restituidos son la aproximación necesaria para calcular el acortamiento (SH) en sistemas compresivos. De la misma manera, los vectores paleomagnéticos permiten controlar las rotaciones de eje vertical (VAR). Cuando SH varía a lo largo de la dirección de una cuña orogénica, con frecuencia se relaciona el gradiente de acortamiento con VAR. Ambas variables se pueden relacionar con modelos trigonométricos sobre el mapa que permiten: 1) corregir el efecto de movimientos fuera de plano que producen errores en la estimación tradicional de SH y 2) calcular la diferencia de acortamiento entre dos cortes geológicos utilizando los valores de VAR. Para controlar VAR, se ha realizado una compilación de datos paleomagnéticos en la Zona Surpirinaica (Sierras Interiores, Cuancas de Jaca-Pamplona y Aínsa y Sierras Exteriores). El área de estudio está limitada por dos cortes geológicos compensadas a escala cortical (Cotiella y Ansó) que atraviesan la cadena en una dirección NNE-SSW, perpendicular a la traza de los principales cabalgamientos. Los datos paleomagnéticos se agrupan en 48 sectores (con entre 4-13 estaciones por sector) que proporcionan una valor robusto de VAR. Los valores de rotación varían entre +1 y +67 dependiendo de la unidad estructural. Asumiendo que la deformación interna es despreciable, los márgenes de error en el cálculo de SH se han estimado teniendo en cuenta los valores de rotación a lo largo de cada corte (modelo 1). Dependiendo de los ángulos de confianza de la rotación (a_{95}) y del promedio de la rotación, los errores de acortamiento varían entre 1% en Ansó a 23% en Cotiella (0.3 y 10.2 km respectivamente). Por otra parte, el gradiente de acortamiento esperado entre las dos secciones se ha calculado a partir de los valores de rotación entre las mismas (modelo 2). El cáculo independiente de SH en la sección de Cotiella, introduce errores de entre 4% a 54% (3.8 y 47.4 km respectivamente) en relación con el acortamiento estimado original (88 km a partir del corte compensado). La estimación de SH depende en gran medida del valor de rotación elegido. Debido a la construcción gráfica de estos modelos, el acortamiento obtenido a partir de los cortes compensados siempre estará sobrestimado.

Palabras clave: gradiente de acortamiento, rotación de eje vertical, corte compensado.

Abstract: Balanced and restored cross-sections are the necessary approach to calculate shortening (SH) in compression regimes and so are paleomagnetic vectors to control vertical axis rotations (VAR). When SH varies along-strike in orogenic wedges this gradient is often connected to the VAR. Both variables have been related in map-view trigonometric models that allow: 1) to correct the effect of out-of-plane movement causing errors on the traditional SH estimation and 2) to calculate the expected difference in shortening between two given sections by using the VAR values. For the purpose to control VAR a compilation of previous paleomagnetic data was carried out in the Southern Pyrenees (Internal Sierras, Jaca-Pamplona and Aínsa basins and the External Sierras front). The study area is bounded by two well-constrained crustal-scale balanced cross-sections (Cotiella and Ansó sections) that crosscut the range in a NNE-SSW direction, perpendicular to the trace of the main thrusts. Paleomagnetic data were grouped in 48 localities (4-13 sites per group) to achieve statistically robust VAR. The rotation values range between +1 and +67 depending upon the structural unit. Assuming internal deformation as negligible, error margins in SH estimates have been calculated using the rotation values measured along both balanced sections (model 1). Depending on the rotation confidence angles (a_{95}) and how we average the varying rotation angle along a cross-section, the SH error may range between 1% in the Ansó section and 23% in the Cotiella section (0.3 and 10.2 km respectively). On the other hand, the expected gradient of shortening was also calculated from the observed VAR between the sections (model 2). The independent calculations of SH in the Cotiella section using the gradient value introduce differences from 4% to 54% (3.8 and 47.4 km respectively) respect to the original shortening estimates (88 km from the cross-section). The different estimation of SH depends greatly on the chosen rotation value, maximum and minimum in that case. Due to the graphical models, the SH value from the balanced cross-sections is always an overestimation of the shortening.

Key words: gradient of shortening, vertical axis rotations, balanced cross-section.

Oliva-Urcia, B. and Pueyo, E.L. (2007): Gradient of shortening and vertical-axis rotations in the Southern Pyrenees (Spain), insights from a synthesis of paleomagnetic data. *Revista de la Sociedad Geológica de España*, 20 (1-2): 105-118.

During the last decades the research on structural geology has focused the problem of deformation in orogenic systems following a 2D approach (Dahlstrom, 1969; Elliott, 1976; Hossak, 1979; Cooper, 1983). Despite the fact 3D restorations techniques are a growing research field (Buddin *et al.,* 1997; Gratier *et al.,* 1991; Rouby *et al.,* 2000; Griffiths *et al.,* 2002; Dunbar and Cook, 2003; Moretti *et al.,* 2005) 2D methods still have a wide interest. The 2D methods, which include cross-section and map-view balancing, are in use due to their simplicity and their ability to validate subsurface interpretations. In any case, the spatial and temporal development of thrust fronts depends on numerous variables, among these: shortening rates, geometry of the sedimentary bodies, mechanical behavior of the pile, syntectonic sedimentation, etc… The development of the compressional deformation may imply the occurrence of confined (near field) or widespread (far field) lateral gradients of shortening and therefore out-of-plane motions across the section. Out-of-plane motions are common in orogenic fronts. Vertical axis rotations are usually associated to the gradients of shortening (McCaig and McClelland, 1992; Allerton, 1998; Wilkerson *et al.,* 2002; Bayona *et al.,* 2003; Sussman *et al.,* 2004). Paleomagnetism has demonstrated to be the best technique to quantify vertical-axis rotations in fold and thrust belts since its first application by Norris and Black (1961) to the Canadian Rockies. Shortening variations along-strike (lateral gradient of shortening) can be trigonometrically related to the vertical-axis rotations in a map-view model of a thrust front (Millán *et al.,* 1996; Pueyo *et al.,* 2004).

The Western part of the Pyrenees is a good example of shortening variation along strike. The available balanced cross-sections in the area display substantial differences of shortening (23 km) along 100 km strike. For that reason numerous paleomagnetic studies have been performed in most structural units during the last years: Internal Sierras; Jaca-Pamplona basin; External Sierras; Aínsa basin and the Cotiella massif. This large dataset has provided vertical-axis rotation magnitudes in an area of about 5000 km^2 bounded by two long cross sections: the Ansó transect (Teixell 1992, 1996) and the Cotiella section (Martínez-Peña and Casas, 2003). In this work we combine the structural and paleomagnetic data by means of map-view models (Pueyo *et al.,* 2004) in order to pursuit two different goals: 1) to evaluate the variation of shortening in relation to the shortening from balanced cross-sections caused by the rotations (out of plane motions) in the Ansó and Cotiella balanced sections. 2) To calculate the shortening value in the eastern section (Cotiella) by using the rotation value and the shortening estimate from the western bound (Ansó) in model 2.

Geological setting

The Pyrenees are a lineal mountain range of double vergence formed by folds and imbricated thrust sheets (Fig. 1A). The eastern part of the belt is constituted by the Pyrenees and the western part is the Basque-Cantabrian Pyrenees (Capote *et al.,* 2002). The limit between both sectors is the Pamplona transfer fault (Larrasoaña, 2000, Capote *et al.,* 2002; Larrasoaña *et al.,* 2003a; 2003b). In a north-south section 5 structural zones are traditionally distinguished (Mattauer and Séguret, 1971, Séguret, 1972): 1) the Aquitain foreland basin to the north is formed due to sediment and tectonic loads (Brunet, 1986). 2) The North Pyrenean Zone is a narrow area of thrusts and folds separated from the Axial Zone by the North Pyrenean Fault Zone. The thrust sheets affecting Paleozoic-Tertiary rocks show both vergences although the vergence towards the north predominates. 3) The Axial Zone involves Paleozoic rocks in an antiformal stack structure in the eastern side of the range, whereas to the west the antiformal stack disappears (Teixell, 1996, 1998). 4) The South Pyrenean Zone is characterized by imbricated thrust sheets and associated folds with a predominantly southern vergence (Séguret, 1972). In the frontal part of the floor basement thrust a series of thrusts emerge and override the sediments of the Ebro foreland basin (Cámara and Klimowitz, 1985). These thrust sheets rise the Marginal Sierras in the South Pyrenean Central Unit (SPCU) and to the west the External Sierras. 5) The Ebro foreland basin store synorogenic sediments ranging in age from Eocene to Miocene (Hogan and Burbank, 1996; Arenas *et al.,* 2001).

Description of the cross-sections

Two balanced cross-sections allows controlling the shortening in the studied area:

Cotiella cross-section

The section is situated in the western part of the Pyrenees (Fig. 1A, B). The structure consists of south verging basement thrust sheets. The basement thrusts include the Gavarnie, Millares, Bielsa, and Guarga thrusts (Martínez-Peña and Casas-Sainz, 2003). The cover units include the South Pyrenean Central Unit (SPCU, Séguret 1972). Within the South-Pyrenean Central Unit, the Montsec and Bóixols units, the Cotiella nappe, and the Serras Marginals thrust sheets are the main structural units (Séguret 1972; Vergés and Muñoz 1990; Muñoz 1992).

In the Axial Zone, the main basement structure is the Gavarnie thrust (Bresson, 1903). The displacement of the Gavarnie thrust decreases towards the east (center of the Pyrenees) being of several hundreds of meters in comparison with the around ten kilometers in the tectonic window with the same name to the west (Soler *et al.,* 1996). The other basement thrusts, Millares and Bielsa, branch together with Gavarnie towards the west. They form the antiformal stack in the Axial Zone in this transect. The Guarga thrust is the

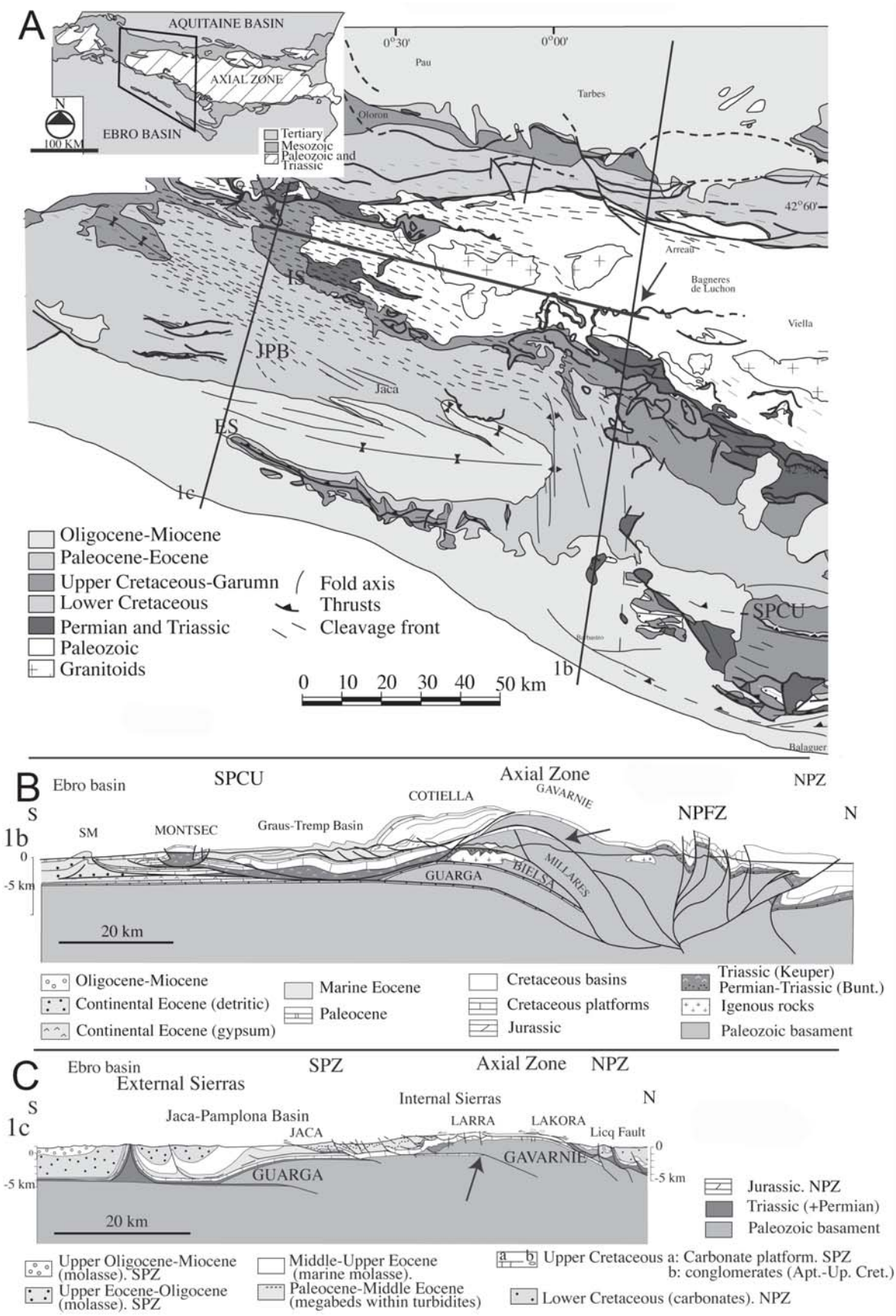

Figure 1.- A) Geological map of the western-central Pyrenees after Choukroune and Séguret (1973). SPCU: South Pyrenean Central Unit. ES: External Sierras. JPB: Jaca-Pamplona piggy-back basin. IS: Internal Sierras. CM: Cotiella Massif. Lines 1b and 1c are the cross-sections below. **B**) Cotiella section from Martínez-Peña and Casas-Sainz (2003). In the cross sections: in capital letters are the name of the thrusts. **C**) Ansó section in the western part from Teixell (1992, 1996) and Teixell and García-Sansegundo (1995), modified in the southern part following and alternative interpretation by Millán (1996). SPZ: South Pyrenean Zone. NPZ: North Pyrenean Zone. NPFZ: North Pyrenean Zone. SPCU: South Pyrenean Central Unit. SM: Serres Marginals.

lowermost thrust of the basement units (Martínez-Peña and Casas, 2003). In relation to the cover thrust sheets, the Cotiella nappe is result of the inversion of a Late Cretaceous basin. The tectonic inversion took place in Early Eocene in conection with the Bóixols thrust towards the east (Martínez-Peña and Casas, 2003). To the south, the Montsec and Serras Marginals thrust sheets show a flat basement top and SW-vergence, detached on the Mesozoic cover (Martínez-Peña and Casas, 2003 and references therein).

The North Pyrenean Zone is characterized by folds and associated axial plane cleavage and steep faults that limit basement blocks (Barrère *et al.,* 1982). The structures show a northward vergence.

The movement of the thrusts in this area follows a foreland breaking sequence (Martínez-Peña and Casas, 2003). First is Gavarnie followed by Millares. The Millares thrust produces the backthrust in the northern segment of the Cotiella thrust sheet. The movement of Bielsa in Cuisian-Lutetian time inverts the Cotiella basin in the south (Séguret, 1972, Garrido-Megías, 1973, Mutti *et al.,* 1988). The displacement of the Bielsa thrust produces shortening in both the Cotiella and Montsec thrust sheets. Finally, Guarga transports the antiformal stack towards the south in the Eocene (Martínez-Peña and Casas, 2003).

The balanced cross-section allows to calculating the shortening in 103 km (Martínez-Peña and Casas, 2003). The shortening in the South Pyrenean Zone calculated from the basement thrusts is about 88 km.

Ansó cross-section

This section shows a similar structure as the other cross-section in the Pyrenees with the exception of the lack of the antiformal stack in the Axial Zone (Fig. 1A, C). The Axial Zone shows a hangingwall anticline in the Gavarnie thrust (Teixell, 1998). Other differences are that the Mesozoic cover here in the west is thinner than in the east, and the divergence in the structures occurs to the north of the Licq fault, whereas more to the east it happens at the NPFZ. The South Pyrenean Zone is represented by series of imbricated thrusts (Larra system) and associated folds with a dominant southerly vergence. The imbricated thrusts affecting Meso-Cenozoic rocks branch to the north of the Axial Zone with the Lakora south-verging basement thrust. The Larra system connects with the Monte-Perdido thrust system towards the east (Souquet, 1967 and Séguret, 1972). The rocks involved in the cover are marls, sandstones and evaporites of Triassic age and carbonatic sediments of Upper Cretaceous and Paleocene age. On top of the platform deposits there is a thin cover (around 60m) of continental deposits followed by 3.500-4.000 m of flysch sediments. The flysch sequence deposits during the Ilerdian- Upper Lutetian (Labaume *et al.,* 1983, Canudo and Molina 1988). Finally, the basin is filled with 3.500-7.000m of continental sediments from Eocene till Miocene times (Soler and Puigdefàbregas, 1970; Puigdefàbregas, 1975; Millán, 1996; Arenas *et al.*, 2001).

These cover thrusts affect the turbiditic sediments in the Jaca-Pamplona basin (Ilerdian- Upper Lutetian, Labaume *et al.,* 1985). The deformation age is between Upper Santonian and the limit between Bartonian and Priabonian (Teixell, 1992). The Larra-Monte Perdido system is deformed by the Gavarnie basement thrust in Priabonian-Chattian times (Teixell, 1992). In the turbiditic basin the first deformation episode (Larra system) produces low angle thrusts. The second deformation episode (Gavarnie thrust) produces thrusts and folds with a southerly vergence (Labaume *et al.,* 1985) and a widespread and penetrative cleavage (Labaume, 1983). The limit to the south of the regional cleavage domain is in the Oturia thrust, although there is locally developed cleavage associated to thrust fronts (Choukroune and Séguret, 1973; Teixell, 1992; Millán, 1996).

To the south of the Jaca-Pamplona basin, the External Sierras are characterized by the Santo Domingo anticline. It is an anticline detached in Keuper facies associated to the Guarga thrust sheet (Pocoví et al., 1990; Millán, 1996; Arenas *et al.,* 2001).

Two deformation stages have been described in the External Sierras: 1) a first one during early-middle Lutetian to early Oligocene times when a series of foreland breaking sequence of thrusts and laterally imbricated towards the west. 2) A second one of Upper Oligocene-Miocene age, when folds and break-back sequence thrusts developed from west to east. In the western side of the External Sierras, Santo Domingo anticline folds the basal thrust together with the footwall-associated ramp (Millán 1996).

The shortening calculated in this transect is 80 km (Teixell, 1998) and the structures in the South Pyrenean Zone accommodate a shortening of 26 km, calculated from the shortening related to the Gavarnie and Guarga basement thrusts.

The paleomagnetic dataset

Paleomagnetism has been extensively applied in the Pyrenees since the early 60's (Van der Lingen, 1960; Schwarz, 1962). Most studies focused on the rotation characterization at both plate and thrust sheet scales but some were devoted to magnetostratigraphy. The western and central sectors of the Pyrenees have one of the highest density of paleomagnetic information: Internal Sierras (Oliva, 2004; Oliva-Urcia and Pueyo 2007); Jaca turbiditic basin (Oms *et al.,* 2003), Jaca molassic basin (Hogan, 1993; Hogan and Burbank, 1996; Pueyo, 2000), Pamplona basin (Larrasoaña *et al.,* 2003a, 2003b); External Sierras (Pueyo *et al.,* 2002, 2003a, 2003b, 2004); Boltaña and Balces anticlines in the External Sierras (Dinarès, 1992; Parés and Dinarès, 1992; Pueyo, 2000; Fernández 2004); Aínsa basin (Bentham 1992; Oms *et al.,* 2006), the Cotiella

massif (Garcés *et al.*, 2005) and the South Central Pyrenean Unit (Dinarès, 1992; Dinarès *et al.*, 1992; Pascual 1992; Pascual *et al.*, 1991, 1992a; 1992b; Galbrun *et al.*, 1993; Serra-Kiel *et al.*, 1994; Meigs, 1995; 1997; Meigs *et al.*, 1996; Beamud *et al.*, 2003 and 2004: López-Martínez *et al.*, 2006). Major findings from this large dataset can be summarized in the following way: no significant rotations were found neither in the frontal thrust sheets of the South Pyrenean Central Unit, nor in the Pamplona basin. These two areas are the limits of our study area (between the Cotiella and Ansó sections). Oblique structures related to the westernmost termination of the SPCU (Aínsa basin and related structures) accommodate large magnitudes of clockwise rotation (more than 70° in the Boltaña and Mediano anticlines). The External Sierras thrust front accommodates a variable degree of clockwise rotation (50°-30°) that seems to be temporally and spatially controlled by the evolution of a complex imbricate thrust system with relatively low lateral propagation velocities, therefore some «border» effects on the rotation magnitude can be expected from the kinematics of this system. A similar but smoother pattern (up to 20° CW) has been recognized in both the Jaca turbiditic basin and in the Internal Sierras. This moderate rotation seems to be connected to the basement kinematics (Guarga or Gavarnie) and not to the cover structures as in the External Sierras. Therefore the rotation can be assumed to reflect a regional lateral variation (gradient) of shortening. Basement paleomagnetic data from Triassic red beds in the Axial Zone are very scarce (Bates, 1989). These data have not been taken into account due to the complexity of interpreting their results. Several components have been described with high errors on the mean values (a_{95}), so we cannot consider them to get a reliable interpretation. Unfortunately the North Pyrenean Zone remains almost unexplored on this ground and therefore any further correction or calculation of shortening has been made exclusively in the southern part of the sections.

Method

Shortening (SH) values coming from balanced cross-sections and vertical-axis rotations (VAR) coming from paleomagnetic sites, have been related in map-view trigonometric models (Pueyo *et al.*, 2004) allowing:

1) to correct the effect of out of plane movement causing errors in the traditional shortening estimation (Fig. 2-model 1); and
2) to calculate the expected difference in shortening between two given sections by using the VAR values (Fig. 3-model 2).

The trigonometric models are a first approximation to calculate the real shortening in a geological cross-section taking into account the effect of the rotation.

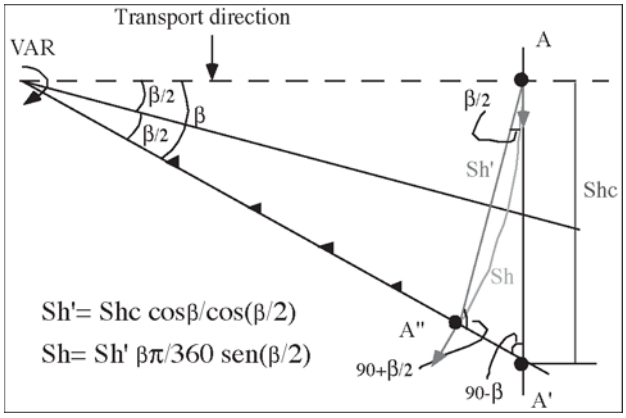

Figure 2.- Trigonometric model used to correct the shortening value of a balanced cross-section knowing the rotation value affecting the same section. Predeformational situation follows line VAR-A. Position of point A after translation and rotation (b) is A. ''The line A-A' represents the position of A after translation to A'. It is the shortening calculated by balanced cross-sections. A good approximation to the real shortening is the line AA'' (Sh') or the arc of that line (Sh). The trigonometric formula is based on the sine rule (see text).

Model 1: Corrected shortening estimate in rotated areas

Assuming internal deformation as negligible, shortening estimates have been calculated using the rotation values along both balanced sections (Fig. 2). In this trigonometric model the point A in the undeformed stage is displaced and rotated towards point A'' after a VAR of b.

The real shortening in the arc (Sh) and in the chord of the arc (Sh') is calculated following the sine law from known angular relationships: Sh'/sen (90-b)= A'-A''/sin b/2=Shc/sin (90+b/2) (sine law), from that we can extract:

$$Sh' = Shc \sin(90-b)/\sin(90+b/2) = Shc \cos b/\cos(b/2)$$

Sh' is the longitude of the arc, to calculate the corresponding chord longitude:

$$Sh = Sh' \, bp/360 \times \sin(b/2)$$

Where Shc is the shortening estimate from the cross-section restoration (classic value), Sh' is the real value of shortening at the chord and Sh is the real shortening at the arc (real path of deformation). In order to extrapolate the trigonometric relationships shown above to estimate the effect of the rotation on the shortening values from the two cross sections, it is necessary that:

1) The transport direction is parallel to the trace of the shortening, although this can be also implemented in the calculations (Pueyo *et al.*, 1999). In our case the section traces can be considered parallel to the transport direction in the northern sector.
2) To know with precision and reliability the vertical axis rotation (b) affecting the cross-

section. This is possible because the extremely high density of paleomagnetic sites: there are more than 4000 samples (around 500 sites) from different magnetostratigraphic profiles and VAR sites. To simplify the calculation and to avoid the influence of extreme cases the study area has been divided in 19 sectors, every sector comprises between 2-12 sites (see compilation in table I and III for the Ansó the Cotiella sections respectively).

3) The classic shortening estimate (Shc) comes from the two selected balanced cross-sections, Ansó (Teixell 1996, 1998) in the western side of the studied area, and Cotiella (Martínez-Peña and Casas 2003) for the eastern side. The line from which the shortening is supposed to be perpendicular it starts in the cut off line of the footwall of the Gavarnie thrust (see arrows in figure 1). The shortening is due to the south-directed displacement of the thrusts and folds. The value of the rotation from the paleomagnetic sectors varies along the cross-section, so one weighted average of the rotation has been calculated for each cross-section.

Model 2: Independent calculation of shortening

The difference in chord length shortening (DS = Sc2-Sc1) between two sections is not only related to the distance between the two sections measured over the footwall (D_{FW}) but is also related to the angle of rotation (Fig. 3):

$$\sin(\beta/2) = (DS/2)/D_{FW};\ (Sc2-Sc1)/2 = D_{FW} \times \sin(\beta/2)$$

The change in the difference of shortening along strike is the shortening gradient (Gs = (Sc1-Sc2) / DFW). The gradient is related only to the amount of rotation associated with the differential movement of the thrust:

$$Gs = (Sc1-Sc2) / D_{FW} = 2 \sin(\beta/2)$$

The most important implication of the shortening gradient is that it allows to calculating by forward modeling a «real» shortening of any cross section without first restoring the stratigraphic series to its pre-deformational form. For example, knowing the shortening in section 1-1' (Sc1) it is possible to calculate the shortening in section 2-2' (Sc2) considering the paleomagnetic rotations between both sections. Conversely, the relationship shown above can be also used to calculate the VAR in an area where the gradient of shortening is known from structural balanced cross-sections.

To calculate the shortening in section 2-2‘ we take: $(Sc2-Sc1)/2 = D_{FW} \times \sin(\beta/2)$, then simply

$$Sc2 = 2\, D_{FW} \times \sin(\beta/2) + Sc1$$

In order to make a prediction of the real shortening, the required data are:

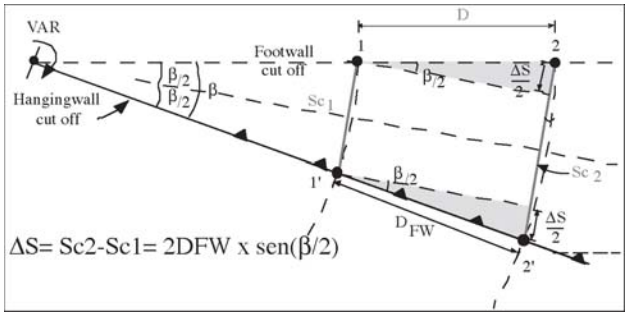

Figure 3.- Trigonometric model to correct the shortening value of a balanced cross-section using a shortening value in another cross-section and the rotation value in the area in between the cross-sections. To calculate shortening in section 2-2‘, the shortening in 1-1‘ and the rotation are used. The grey areas are the difference in shortening between these two sections, marked as DS/2. The trigonometric relationship can be: $(DS/2)/D = \tan(\beta/2)$ or $(DS/2)/D_{FW} = \sin(\beta/2)$. D is the distance between the cross-sections before the deformation, and D_{FW} is the distance between both cross sections measured along the footwall cutoff.

1) the magnitude of rotation (β) in the area between the two sections
2) reliable shortening value along a line of section where the positions of both cutoffs are known.
3) the distance between both cross sections measured along the footwall cutoff (D_{FW}) over the geological map.

For instance, given a corrected shortening at cross section 1 (Sc1), a realistic minimum shortening value for cross section 2 (Sc2) can be determined even if the hanging wall cutoff has been eroded (Fig. 3):

$$Sc2 = Sc1 + DS = Sc1 + 2\, D_{FW} \sin(\beta/2)$$

This model has been applied in the Southern Pyrenees as seen in figure 5.

Results and discussion

Application of model 1: Corrected shortening estimate in rotated areas (Fig. 4)

Ansó cross-section:

To calculate one weighted rotation value for the section, the rotation values distributed along the cross-section are divided in two sectors: the northern part with a length of 39.5 km, from the Internal Sierras till the northern border of the Guarga Sinclinal, and the southern part, of 14.2 km in the molassic Jaca-Pamplona basin and External Sierras. The average clockwise rotation of the northern part is +16º. The average value has been extrapolated to the turbiditic Jaca-Pamplona basin. The southern part shows a rotation value of +34º. For the whole section the calculated weighted average is: +21º= [(39.5x16) + (14.2x34)]/53.7.

With the rotation we calculate the shortening in the chord of the arc:

$$Sh' = Shc \cos\beta / \cos(\beta/2) = 26 \cos 21^{o} / \cos 10.5^{o} = 24.6 \text{ km}$$

ANSO	D&I	α 95	k	β	Number of sepecimens	age	references
75. Sª Bernera	21 , 47	5	75	+16	101	Upper Cretaceous	Oliva and Pueyo, 2007
9. Yesa	21 , 51	13	19	+16	57	Eocene	Pueyo, 2000
14. Bagüés	17 , 18	13	5	+12	33	Upper Eoc.-Oligoc.	Hogan, 1993
16. Sta. Bárbara (N)	21 , 34	10	14	+16	17	Upper Eoc.-Oligoc.	Pueyo, 2000
12. S. Marzal (N)	30 , 55	20	9	+25	6	Bartonian	Pueyo, 2000
18. Sto. Domingo (N)	47 , 40	10	14	+42	16	Bartonian	Pueyo, 2000

Table I.- D&I: declination, inclination. a95 and k statistical parameters. b: registered rotation. Number of specimens used to calculate the average. Age of the samples. Original work where the data come from.

Ansó-Arzacq	Shc (km)	Sh' (chord) km	Sh (arc) km	β	error
Minimum	26	25.7	25.7	+10º	1%
Medium	26	24.6	24.7	+21º	5%
Maximum	26	22.9	23.2	+32º	11%

Table II.- See text for details: Summary table for the calculations using model 1 in the Ansó section. b: rotation.

Figure 4.- Application of model one in the Southern Pyrenees. Cones of rotation of mean values used with the a_{95} (see text for more details) are represented together with the errors in the shortening values. The weighed rotation for each part of the section is noted. The tables I and III show the data and the samples per cone. Tables II, IV and V show the results of the calculations.

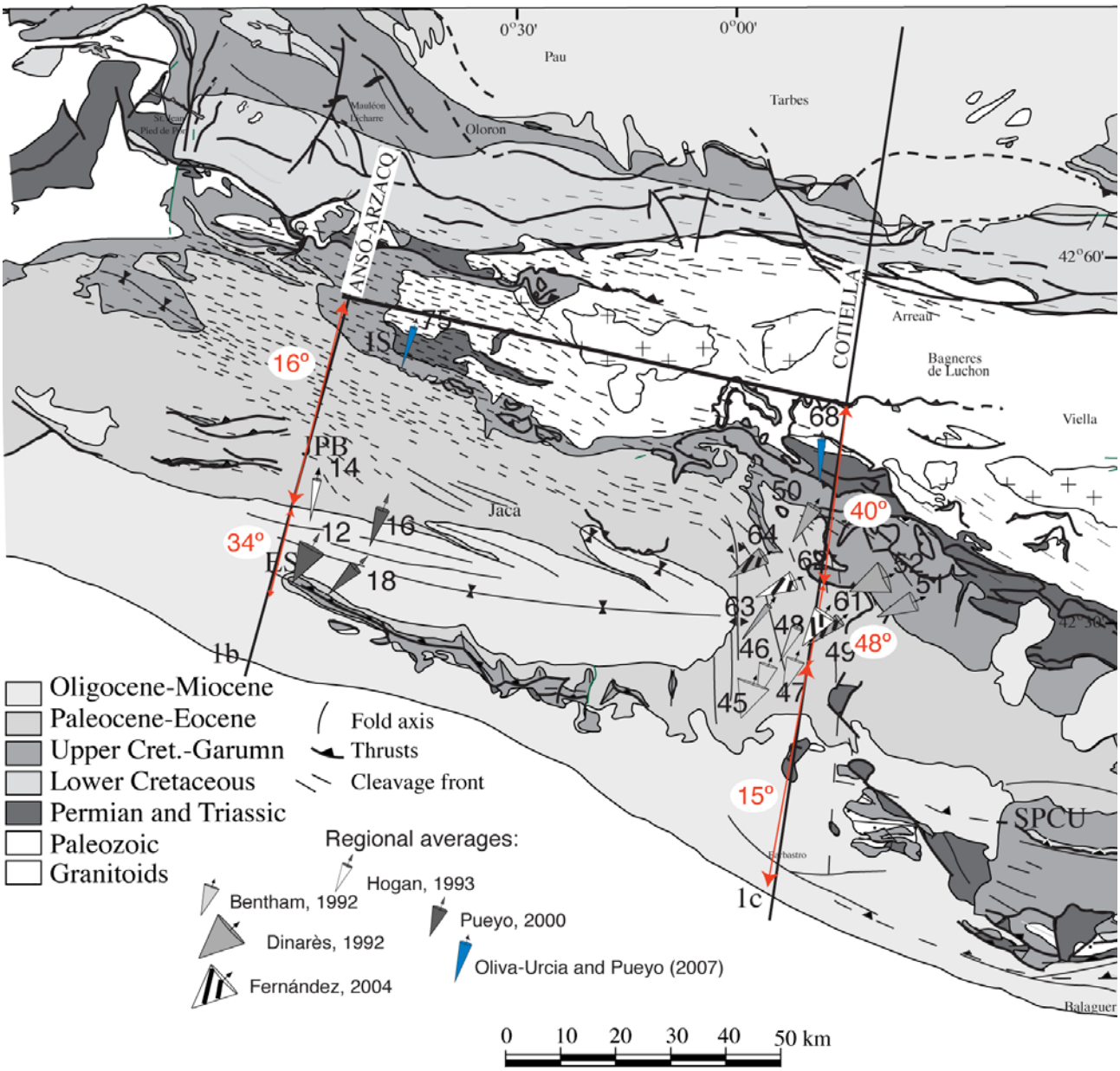

COTIELLA	D&I	α 95	k	β	Number of sepecimens	age	references
68. Bielsa	6 , 37	5	46	+1	150	Triassic	Oliva 2004
50. 90J-32+33+34+35	38 , 28	11	55	+33	14	Ypresian	Dinarès, 1992
52. 90J-27-28	65 , 46	23	61	+60	8	Ypresian	Dinarès, 1992
51. 90J-13+14+22+23	72 , 55	14	36	+67	21	Ypresianse	Dinarès, 1992
62. CB+SB+GB	69 , 54	13	59	+65	23	Early Lutetian	Fernández, 2004
64. YB+BB+90J39	61 , 43	12	68	+57	19	Ilerd.-Ypres.	Dinarès1992, Fernández 2004
63. 90J38+25	43 , 25	4	2383	+39	6	Lutetian	Dinarès, 1992
61. EM1-PM1-SM1	34 , 45	17	37	+29	20	Mid.-Late Lutetian	Fernández, 2004
49. 90J-36-31+FM1-2-3-4+YM1-2	54 , 49	9	32	+50	60	Ypres.-Lutetian	Dinarès1992,Fernández 2004
48. Mediano	22 , 53	6	14	+22	92	Late Eoc. - Oligocene	Bentham, 1992
	212 , -25	15	9				
47. Ligüerre	12 , 51	12	9	+16	58	Mid.-Late Eocene	Bentham, 1992
	209 , -54	15	8				
46. Eripol	34 , 54	8	12	+14	63	Late Eocene – Oligoc.	Bentham, 1992
	184 , -20	21	6				
45. Almazorre	2 , 48	25	8	+15	18	Bartonian	Bentham, 1992
	218 , -24	32	8				

Table III.- Same legend as in table I.

And the length of the arc is:

Sh=Sh' bp/360 sen (b/2) = 24.6 x 21º x ð/360 sen 10.5º = 24.7 km

Due to the fact that rotations values have an associated error (a_{95}), we calculate the error for the section: 11º

Then, the shortening and the weighted error are involved in the calculation of the shortening error. With a maximum rotation value (32º) the error would be:

Sh'= Shc cosb/cos (b/2)= 26 cos32º/cos16º = 22.9 km in the chord; and in the arc: Sh=Sh' bp/360 sin (b/2)= 22.9 x 32º x p/360 sin 16º = 23.2 km.

And the shortening error for the minimum rotation value (10º):

Sh'= Shc cosb/cos (b/2)= 26 cos 10º/cos 5º = 25.7 km in the chord; and in the arc: Sh=Sh' bp/360 sin (b/2)= 25.7 x 10º x p/ 360 sin 5º = 25.7 km.

The calculated values are compiled in table II together with the error in the shortening calculation respect to the shortening from the balanced cross-section. With this approach, the shortening values depend on the taken rotation value. The calculation of the shortening with VAR closer to the shortening values from the balanced cross-section is the one with the lower rotation (10º).

Cotiella	Shc (km)	Sh' (chord) km	Sh (arc) km	β	error
Minimum	88	85,7	85,9	+15º	2%
Medium	88	78,8	79,7	+30º	10%
Maximum	88	67,5	67,8	+45º	23%

Table IV.- Same legend as in table II (see text).

Cotiella cross-section:

The rotation values used in this section are compiled in table III, see also figure 4 for the map view.

In this case the section is divided in three sectors: the Axial Zone and Internal Sierras: 39 km with +40º of averaged rotation; the northern side of the Aínsa basin: 15 km with +48º of rotation, and the southern side with 47 km and +15º of rotation. The averaged rotation for the whole section is: ((39km x 40º)+(15 km x 48º)+(47km x 15º))/101 km = +30º.

The weighted error for the rotation is: 15º.

The shortening error is maximum when: Sh'= Shc cos b /cos (b/2)= 88 cos 45º/cos23º=67.5 km. In the arc is: Sh=Sh' bp/360 sin (b/2)= 67.5 x 45º x p/360sin 23 = 67.8 km.

The shortening error is minimum in the chord when: Sh'= Shc cos b/cos (b/2)= 88 cos 15º/cos 7.5º = 85.7 km. In the arc: Sh= Sh' bp/360 sin (b/2)= 85.8 x 15º x p/ 360sen 7.5º= 85.9 km.

The averaged error in the shortening is for the chord: Sh = Shc cosb/cos (b/2) = 88 cos30º/cos15º = 78.8 km. In the arc: Sh=Sh' bp/360 sin (b/2) = 78.8 x 30 x p/360 sin 15 = 79.7 km. The calculations are sum up in table IV, where again, the calculation with VAR closer to the shortening calculated by means of the balanced cross-section, is the one with the lowest rotation value.

For the two sections the summary of the shortening errors are in table V, where Shc is the shortening from the balanced cross-sections and Sh the shortening corrected with the rotation (in the arc), the mean value and in brackets the minimum and maximum shortening values obtained from the respective rotation values.

These corrections predict shortening value overestimations between 1-23% if *out-of-plane*

	ANSÓ	COTIELLA
Shc	26 km	88 km
Sh	24.7 km (23.2-25.7)	79.7 km (67.8-85.9)
error	5% (1%-11%)	10% (2%-23%)

ROTATIONS BETWEEN SECTORS

Table V.- Summary table for model 1 in the Southern Pyrenees.

motions (vertical axis rotations) are not considered. The lowest error (1%) is in section 1, when the value of the rotation is the lowest. The 23% implies a difference of shortening in with the cross-section 2 of 20.2 km when the maximum rotation value is used.

It is worth to mention that these overestimations can camouflage the real rotation value; on one hand the calculated rotation implies a smoothing effect on the process of averaging. On the other hand, in the case the rotation has been only partially determined by paleomagnetic analysis (e.g. synrotational sedimentation), the lower sedimentary pile is not able to record the whole rotation value because the magnetization is blocked after rotation starts, so that the magnetization vector does not account for the total rotation value.

Application of model 2: Independent calculation of shortening (Fig. 5)

The shortening in Cotiella section can be independently calculated from the corrected shortening in the Ansó section and the rotation values obtained

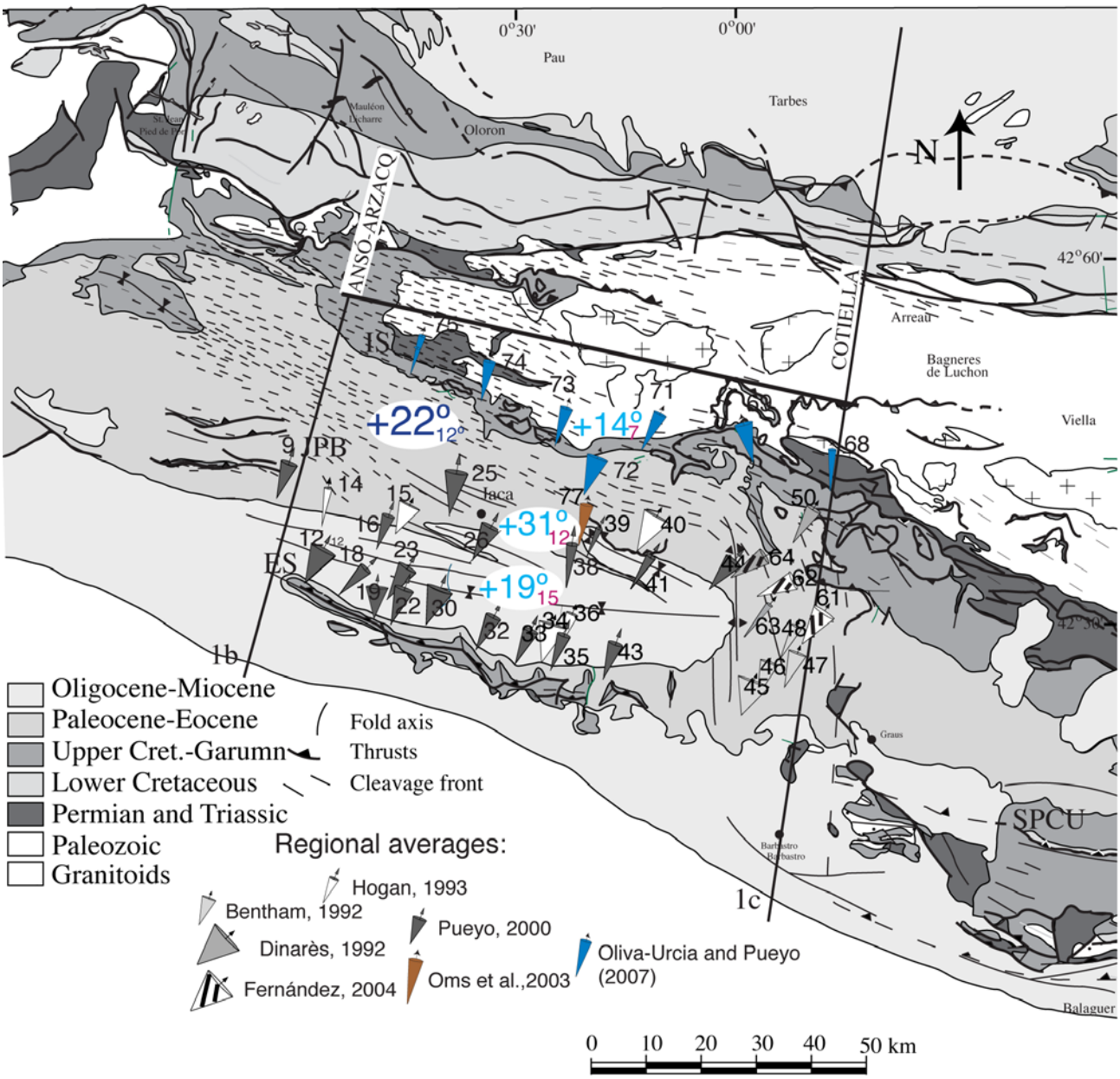

Figure 5.- Application of model two in the Southern Pyrenees. The cones represent the averaged of the sites for that point, with the a_{95}. The weighed rotation for the three surfaces (SP1: Internal Sierras, SP2: Jaca-Pamplona basin, SP3: External Sierras), in light blue and the corresponding error in the rotation in purple see table 6. The weighted rotation for the whole surface between the cross-sections and its error is also shown in dark blue. The table shows the errors of the shortening in the east section considering different shortenings in the west sector; in addition, different rotations have been used depending on the a_{95}.

ANSÓAND COTIELLA		km2	rotation	α_{95}
Mean of SP1	74,75, 73, 72, 71, 69, 68, 50	1843	+14	7
Mean of SP2	9, 14, 16, 15, 25, 26, 38, 77, 39, 40, 41, 44, 64, 62, 63, 61, 48	2116	+31	12
Mean of SP3	12, 18, 19, 23, 22, 30, 32, 33, 34, 35, 43, 45, 46, 47	2458	+19	15
	TOTAL surface	6417		
	weighted mean		+22	12

Table VI.- Model 2 in the Southern Pyrenees.

from paleomagnetic studies in the area between both transect. The Ansó section has been chosen as simpler if compared with Cotiella since it appears to have less structural uncertainty The erosion in the west can be considered lower and the structures are better preserved, therefore the shortening value is likely more accurate than the Cotiella estimation. With respect to the paleomagnetic data 48 sites in the area between both sections have been used (see table VI and table in the annex for details).

The rotation is weighted now for the surface (instead of the length) in three sectors between the two sections. SP1 correspond to the area between the Axial Zone and the Internal Sierras. SP2 correspond to the Jaca-Pamplona basin and SP3 to the External Sierras. The numbers in this table VI correspond to the sectors shown in figure 5 and the annex table.

By means of the corrected values for the shortening in the Ansó section (25.7; 24.7 and 23.2 km), we can calculate the expected shortening in the Cotiella transect. This independent calculation can be, once more, implemented considering the mean weighted rotation magnitudes together with the respective error (deduced from the a_{95}). Only the maximum values predicted in our calculations seem to fit with the estimated by cross restoration (see table VII). This observation points to an overestimation of shortening caused by the important out-of-plane motions associated to the Boltaña, Balces and Mediano anticlines. As can be easily deduced from our map-view models, shortening estimates from classic restoration techniques will be always overestimated in a magnitude directly dependent on the rotation value; that is the shortening gradient (Pueyo *et al.*, 2004).

As it happens in the application of model 1, in model 2 the shortening estimation is highly dependant on: 1) the accuracy of the rotation determination. 2) The age of this rotation since this could imply underestimation when synrotational sedimentation takes place. 3) In addition, the selected transects because of the assumptions involved on the balanced cross-sections (e.g. if erosion force to interpret the situation of cutoffs). In our case the most important gradient of shortening, as expectable, seems to be associated to the area of oblique structures between the Jaca and the Aínsa basins.

Sh1 (arc) km	Minimum (10°) km	Medium (22°) km	Maximum (34°) km
25.7	43.1 (51%)	44.9 (49%)	84.2 (4%)
24.7	42.1 (52%)	43.9 (50%)	83.2 (6%)
23.2	40.6 (54%)	42.4 (52%)	81.7 (7%)

Table VII.- Summary table for model 2 in the Southern Pyrinees.

Conclusions

The paleomagnetic information available in the Southern Pyrenees together with the map-view trigonometric models (Pueyo *et al.*, 2004) have allowed us evaluating the margins of error of the shortening estimations in the southern portion of two orogenic scale transects; the Ansó (Teixell, 1996) and Cotiella (Martiñez-Peña and Casas, 2003) sections.

The corrected shortening values (model 1) display errors between 1-23 % (minimum and maximum rotation values in Ansó and Cotiella sections respectively) when compared with the shortening deduced by classic restoration. An independent calculation of shortening for the Cotiella transect (model 2) considering the Ansó shortening and the VAR between both sectors, predicts important differences (4-54%) when compared with the classic restoration deductions. In this case the bigger difference is due to the minimum chosen rotation value for the calculation. The classic restoration will always overestimate the real shortening. The errors depend greatly in the accuracy of the rotation values and in the time the rotation takes place. A refinement of the rotation data from the Central-Western Pyrenees and the rotation model will result in a more accurate calculation of the shortening values.

Acknowledgements

B. Oliva thanks for a grant from the Aragonaise Government and a postdoctoral Scholarship from the Spanish Ministry of Science (MEC). E. L Pueyo is funded by a Ramón y Cajal Young Research Contract (MEC). Other research funding comes from the projects BTE 2002-04168, CGL*2006-2289-BTE* (MEC) and Geokin3DPyr (CTPR04/2005- INTERREG IIIa- European Council). We thank Dr. Antoni Teixell and an anonymous reviewer for their comments to improve the manuscript.

References

Allerton, S. (1998): Geometry and kinematics of verti-cal-axis rotations in fold and thrust belts. *Tectonophysics*, 299: 15-30.

Arenas, C., Millán, H., Pardo, G. y Pocoví A. (2001): Ebro Basin continental sedimentation associated with late compressional Pyrenean tectonics (north-eastern Iberia); controls on basin margin fans and fluvial systems. *Basin Research,* 13 (1): 65-89. 2001.

Barrère, P., Bouquet, C., Debroas, J., Pélissonnier, h., Peybérnes, B., Soulé, J-C., Souquet, P., Ternet, Y. (1982): *Carte géologique de la France* (1/50.000), sheet Arreau (1072)-Orléans. Boureau de recherches géologiques et minières, Orléans.

Bates, M.P. (1989): Palaeomagnetic evidence for rota-tions and deformation in the Nogueras Zone, central southern Pyrenees, Spain. *Journal Geological Societym, London* 146: 459–476.

Bayona, G., Thomas, W. A. y Van der Voo, R. (2003): Kinematics of thrust sheets within transverse zones: a structural and paleomagnetic investigation in the Appalachian thrust belt of Georgia and Alabama. *Journal of Structural Geology,* 25: 1193–1212.

Beamud, B., Garcés, M., Cabrera, Ll., Muñoz, J.A. y Almar, Y. (2003): A new middle to late Eocene continental chronostratigraphy from NE Spain. *Earth and Planetary Science Letters,* 216: 501-514.

Beamud, E., Garcés, M., Muñoz, J.A., Cabrera, Ll. y Almar, Y. (2004): Distribución de las rotaciones paleomagnéticas en la cuenca de Graus-Tremp durante el Terciario. *Geotemas,* 6 (4): 283-286.

Bentham, P.A. (1992): *The tectono-stratigraphic development of the western oblique ramp of the south-central Pyrenean thrust system, Northern Spain.* Ph.D. University of Southern California, 253p.

Bresson, A. (1903): Études sur les formations anciennes des Hautes et des Basses Pyrénées (Haute Chaine). Bulletin Service *Carte géologique, France*. XIV-93: 45-322. XIV-93: 45-322.

Brunet, M.F. (1986): The influence of the evolution of the Pyrenees on adjacent basins. *Tectonophysics*, 129 (1-4): 343-354.

Buddin, T.S., Kane, S.J., Williams, G.D. y Egan S. S. (1997): A sensitivity analysis of 3-dimensional restoration techniques using vertical and inclined shear constructions. *Tectonophysics*, 269, 1-2: 33-50.

Capote, R., Muñoz, J.A., Simón, J.L., Liesa, C.L. y Arlegui, L.E. (2002): Alpine tectonics I: the Alpine system north of the Betic Cordillera. In: *Geology of Spain* (W. Gibbons y T. Moreno, Eds.). Geological Society London: 367-400.

Choukroune, P. y Séguret, M. (1973): Carte Structurale des Pyrénées. ELF-ERAP. Mission France. Boussens.

Cámara, P. y Klimowitz, J. (1985): Interpretación geodinámica de la vertiente centro-occidental surpirenaica (cuencas de Jaca-Tremp). *Estudios Geológicos*, 41: 391-404.

Cogne, J.P. (1987): Paleomagnetic direction obtained by strain removal in the Pyrenean Permian redbeds at the «Col du Somport» (France). *Earth and Planetary Science Letters*, 85 (1-3): 162-172.

Cooper, M.A. (1983): The calculation of bulk strain in oblique and inclined balanced sections. *Journal of Structural Geology*, 5 (2): 161-165.

Dahlstrom, C.D. (1969): Balanced cross-sections. *Canadian Journal of Earth Sciences*, 6: 743-757.

Dinarès, J. (1992): *Paleomagnetisme a les Unitats Sudpirinenques Superiors. Implicacions estructurals.* Tesis doctoral, Univ. de Barcelona, 462 p.

Dinarès, J.; McClelland, E. and Santanach, P. (1992): Contrasting rotations within thrust sheets and ki-nematics of thrust tectonics as derived from palaeomagnetic data: an example from the Southern Pyrenees. In: *Thrust tectonics* (K.R. McClay, Ed.). Chapman & Hall Eds., 265-276.

Dunbar, J.A. y Cook, R.W. (2003): Palinspastic reconstruction of structure maps:an automated finite element approach with heterogeneous strain. *Journal of Structural Geology*, 26: 1021–1036.

Elliott, D. (1976): The motion of thrust sheets. *Journal of Geophysical Research*, 81: 949-963.

Fernández, O. (2004). Reconstruction of geological structures in 3D. An example from the Southern Pyrenees. Tesis doctoral, Univ. de Barcelona, 321p.

Galbrun,B., Feist, M., Colombo, F, Rocchia, R. y Tamabareau, Y. (1993): Magnetostratigraphy and biostratigraphy of Cretaceous-Tertiary continental deposits, Ager Basin, Province of Lerida, Spain. *Paleogeography, Paleoclimatology, Paleoecology,* 102: 41-52.

Garcés, M., J. García-Senz, J.A. Muñoz y E. Beamud (2005): Shallow and deep burial remagnetisations in the Cotiella Massif (late Cretaceous, South Central Pyrenees): insights from rock magnetic properties. *Geophysical Research Abstracts,* 7, 04069.

Garrido-Megías, A. (1973): *Estudio geológico y relación entre tectónica y sedimentación del Secundario y Terciario de la vertiente meridional pirenaica en su zona central (Provincias Huesca y Lérida).* Tesis doctoral, Univ. de Granada, 395 p.

Gratier, J.P, Guillier, B., Delorme, A. y Odonne, F. (1991): Restoration and ba-lance of a folded and faulted surface by best-fitting of finite elements; principle and applications. *Journal of Structural Geology,* 13 (1): 111-115.

Griffiths, P., Jones, S., Salter, N., Schaefer, F., Osfield, R. y Reiser, H. (2002): A new technique for 3-D flexural-slip restoration. *Journal of Structural Geology*, 24: 773-782.

Hogan, P.J. (1993): *Geocrohonologic, tectonic and stratigraphic evolution of the Southwest Pyrenean foreland basin, Northern Spain.* PhD Thesis. Univ. of Southern California, 219 p.

Hogan, P.J. y Burbank D.W. (1996): Evolution of the Jaca piggyback basin and emergence of the External Sierra, southern Pyrenees. In: *Tertiary ba-sins of Spain* (P.F. Friend and C.J. Dabrio, Eds.). Cambridge Univ. Press, 153-160.

Hossak, J.R. (1979): The use of balanced cross-sections in the calculation of orogenic contraction: a review. *Jouurnal Geological Society, London,* 136: 705-711.

Labaume, P. (1983): *Evolution tectono-sédimentaire et mégaturbidites du bassin turbiditique eocene sud-pyrénéen (entre les transversales Col du Somport-Jaca et Pic d'Orhy-Sierra de Leyre).* USTL, Montpellier. Thèse 3ème cycle, 170 p.

Labaume, P., Séguret, M. y Seyve, C. (1985): Evolution of a turbiditic foreland basin an analogy with an accretionary prism: Example of the Eocene South-Pyrenean basin. *Tectonics*. 4 (7): 661-685.

Larrasoaña, J. C. (2000): *Estudio magneto-tectónico de la zona de transición entre el Pirineo central y occidental: implicaciones estructurales y geodinámicas.* Tesis doctoral Univ. de Zaragoza. 287 p.

Larrasoaña, J. C., Parés, J. M., Millán, H., del Valle, J. y Pueyo, E.L. (2003a): Paleomagnetic, structural, and stratigraphic constraints on transverse fault kinematics during basin inversion: the Pamplona fault (Pyrenees, north Spain). *Tectonics*, 22 (6) 1071. doi: 10.1029/2002TC001446.

Larrasoaña, J. C, Parés, J.C., del Valle, J. y Millán, H. (2003b): Triassic paleomagnetism from the Western Pyrenees revisited: implications for the Iberian–Eurasian Mesozoic plate boundary. *Tectonophyisics*, 362, (1-4): 161-182.

López-Martínez N., Dinarès-Turrell J., Elez-Villar J. (2006): Chronostratigraphy of the continental paleocene series from the South Central Pyrenees (Spain): New magnetostratigraphic constraints. *Proceeding of the Climate and Biota of the Early Paleocene.* Volume abstract, Bilbao.

Martínez-Peña, M.B. y Casas-Sainz A.M. (2003): Cretaceous-Tertiary tectonic inversion of the Cotiella Basin (Southern Pyrenees, Spain). *International Journal of Earth Sciences (Geol. Rundsch.),* 92: 99-113.

Mattauer, M. y Séguret, M. (1971): Les relations entre la chaine des Pyrénées et le golfe de Gascogne. En: *Histoire structurale du Golfe de Gascogne*: 1-24.

McCaig, A.M. y McClelland, E. (1992): Palaeomag-netic techniques applied to thrust belts. In: *Thrust Tectonics* (K.R. McClay, Ed.). Chapman y Hall, 209-216.

Meigs, A. J. (1995): *Thrust faults, thrust sheets, and thrust-belts; new insights from the Spanish Pyrenees.* PhD Thesis, Univ. of Southern California, 275 p.

Meigs, A. J. (1997): Sequential development of selected Pyrenean thrust faults. *Journal of Structural Geology,* 19 (3-4): 481-502.

Meigs, A. J., Vergés, J. y Burbank, D.W. (1996): Ten-million-year history of a thrust sheet. *Geological Society of America Bullettin*, 108 (12): 1608-1625.

Millán, H. (1996): *Estructura y cinemática del frente de cabalgamiento surpirenaico en las Sierras Exteriores Aragonesas*. Tesis Doctoral, Univ. de Zaragoza, 330 p.

Millán, H., Pueyo, E.L. y Pocoví, A. (1996): Estimación del acortamiento en áreas afectadas por rotaciones y su contrastación con datos paleomagnéticos. *Geogaceta,* 20 (4): 755-758.

Moretti, I., Lepage, F. y Guiton, M. (2005): KINE3D: A new 3D restoration method based on a mixed approach linking geometry and geomechanics. *Oils & Gas Science and Technology (Rev IFP*), 60: 1-12.

Muñoz, J.A. (1992): Evolution of a continental collision belt: ECORS-Pyrenees crustal balanced section. En: *Thrust tectonics* (McClay, Ed.). Chapman y Hall, 235-246.

Mutti, E., Séguret, M. y Sgvavetti, M. (1988): Sedimentation and deformation in the Tertiary sequences of the southern Pyrenees. Guidebook 7, *American Association of Petrology*, Geology of the Mediterranean Basins Conference, Nice.

Norris, D.K. y Black, R.F. (1961): Application of palaeomagnetism to thrust mechanics. *Nature,* 192: 4806, 933-935.

Oliva, B. (2004): *Geometría y cinemática rotacional en las Sierras Interiores y Zona Axial (sector de Bielsa) a partir del análisis estructural y paleomagnético*. Tesis doctoral, Univ. de Zaragoza, 290 p.

Oliva, B. y Pueyo, E.L. (2007): Rotational basement kinematics deduced from remagnetized cover rocks (Internal Sierras, southwestern Pyrenees). *Tectonics*, 26: TC4014, doi:10.1029/2006TC001955.

Oms, O., Babault, J., Dinarès-Turell, J., Rouby, D., Remacha, E, Eichenseer, H., Urreiztieta, M., Nalpas, T. (2006): Validación de modelos geológicos y magnetotectónica. Ejemplo en la Cuenca Surpirenaica Central. En: *MAGIBER I: Paleomagnetismo en la Península Ibérica (*M. Calvo, M. Garcés, C. Gomes, J.C. Larrasoaña, E. Pueyo y J.J. Villalaín, Eds.). Universidad de Burgos, 41-44.

Oms, O., Dinarès-Turel, J. y Remacha, E. (2003): Magnetic stratigraphy from deep clastic turbidites: an example from the Eocene Hecho group (southern Pyrenees). *Studia Geophysica Geodetica,* 47: 275-288.

Parés, J.M. y Dinarès-Turell, J. (1993): Magnetic fabric in two sedimentary rock types from the Southern Pyrenees. *Journal of Geomagnetism and Geoelectricity*, 45, 193-205.

Paris, J.P., Vernet, R., Bixel, F., Icole, M., Choukroune M.P. y Pyolle, J. (1975): *Carte géologique de la France* (1/50.000), sheet Montréjeau (1054). Bureau de recherches géologiques et minières, Orléans.

Pascual, O. (1992): *Magnetoestratigrafía del estratotipo y paraestratotipo del Ilerdiense, seciones de Tremp y Campo (Cuenca de Tremp-Graus).* Tesis doctoral, Univ. Autònoma de Barcelona, 461 p.

Pascual, J.O., Pares, J.M. y Garcés, M. (1992a): Magnetoestratigrafia y bioestratigrafia del Eoceno inferior; seccion de Campo (provincia de Huesca). En: *Actas del Congreso Latinoamericano de Geologia,* 8: 164-169.

Pascual, J.O., Samsó, J.M., Tosquella, J., Pares, J.M. y Serra-Kiel, J. (1991): Magnetoestratigrafia y bioestratigrafia del estratotipo del Ilerdiense (Tremp, Lleida). In: *I congreso del Grupo Español del Terciario* (F. Colombo, E. Ramos-Guerrero y S. Riera, Eds). Congreso del Grupo Español del Terciario, 244-247.

Pascual, O., Parés, J.M., Langereis, C.G. y Zijderveld, J.D.A. (1992b): Magnetoestratigraphy and rock magnetism of the Ilerdian stratotype at Tremp, Spain. *Physics of the Earth and Planetary Interiors,* 74: 139-157.

Pocoví, A., Millán, H., Navarro, JJ. y Martínez, M.B. (1990): Rasgos estructurales de la Sierra de Salinas y zona de los Mallos (Sierras Exteriores, Prepirineo, provincias de Huesca y Zaragoza). *Geogaceta,* 8: 36-39.

Pueyo, E. L. (2000): *Rotaciones paleomagnéticas en sistemas de pliegues y cabalgamientos. Tipos, causas, significado y aplicaciones (ejemplos del Pirineo Aragonés).* Tesis doctoral, Univ. de Zaragoza, 296 p.

Pueyo, E. L., H. Millán, H. y Pocoví, A. (1999): Determination of shortening in rotated areas by means of magneto-tectonic and trigonometric analysis, preliminary results. *Proceeding of the Thrust Tectonic Meeting* (K.R. McClay, Ed.): 294-300.

Pueyo, E. L., Millán, H. y Pocoví, A. (2002): Rotation velocity of a thrust: a paleomagnetic study in the External Sierras (Southern Pyrenees). *Sedimentary Geology*, 146: 191–208.

Pueyo, E.L., Parés, J.M., Millán, H. y Pocoví, A. (2003a): Conical folds and apparent rotations in paleomagnetism (A case studied in the Southern Pyrenees). *Tectonophysics*, 362 (1-4): 345-366.

Pueyo, E. L., Pocoví, A., Millán, H. and Sussman, A.J. (2004): Map-view models for correcting and calculating shortening estimates in rotated thrust fronts using paleomagnetic data. En: *Orogenic Curvature: Integrating Paleomagnetic and Structural Analyses* (A.J. Sussman y A.B. Weil, Eds). Geological Society of America Special Publication, 383: 57-71.

Pueyo, E.L., Pocoví, A., Parés, J.M., Millán, H. y Larrasoaña, J.C. (2003b): Thrust ramp geometry and spurious rotations of paleomagnetic vectors. *Studia Geophysica Geodetica,* 47: 331-357.

Rouby, D., Xiao, H. y Suppe, J. (2000): 3-D restoration of complexly folded and faulted surfaces using multiple unfolding mechanisms. *AAPG Bulletin*, 84: 805–829.

Schwarz, E. J. (1962): *Geology and paleomagnetism of the valley of the Río Aragón Subordan north and east of Oza.* (PhD Thesis, University of Utrecht). Estudios Geológicos, 18: 193-240.

Séguret, M. (1972): *Etude tectonique des nappes de series décollées de la partie centrale du versant sud des Pyrénées. Caractère synsédimentaire, rôle de la compression et de la gravité*. Thèse Doct. Publ. USTELA. Série Géol. Montpellier. 155 p.

Serra-Kiel, J., Canudo, J.I., Dinarès, J., Molina, E., Ortiz, N., Pascual, J.O., Samso, J.M. y Tosquella, J. (1994): Cronoestratigrafía de los sedimentos marinos del Terciario inferior de la Cuenca de Graus-Tremp (Zona Central Surpirenaica). *Revista de la Sociedad Geológica de España,* 7: 273-297

Soler, M. y Puigdefàbregas, C. (1970): Líneas generales de la geología del Alto Aragón occidental. *Pirineos.* 96: 5-19.

Soler, D., Teixell, A. y García-Sansegundo, J. (1996): Amortissement latéral du chevauchement de Gavarnie et sa relation avec les unités sud-pyrénéennes. *Comptes Rendus Académie Sciences Paris*, 327: 699-704.

Souquet, P. (1967): Le Crétacé supérieur sudpyrénéen en Catalogne, Aragon et Navarre. Thèse d'Etat, Univ. de Toulouse, 529p.

Sussman, A.J., Butler, R.F., Dinarès-Turell, J. y Vergés, J. (2004): Vertical-axis rotation of a foreland fold and implications for orogenic curvature: an example from the Southern Pyrenees, Spain. *Earth and Planetary Science Letters*, 218: 435-449.

Teixell, A. (1992)*: Estructura alpina en la transversal de la terminación occidental de la Zona Axial pirenaica.* Tesis doctoral, Univ. de Barcelona., 252p.

Teixell, A. (1996): The Ansó transect of the southern Pyrenees: basement and cover thrust geometries. *Journal of Geophysical Research*, 102: 20.325-20.342.

Teixell, A. (1998): Crustal structure and orogenic material budget in the west central Pyrenees. *Tectonics*, 17 (3): 395-406.

Teixell, A. y García-Sansegundo, J. (1995): Estructura del sector central de la Cuenca de Jaca (Pirineos meridionales). *Revista de la Sociedad Geológica de España*, 8(3): 215-228.

Van der Lingen, G. J. (1960): Geology of the Spanish Pyrenees, north of Canfranc, Huesca province. (PhD Thesis, University of Utrecht). *Estudios Geológicos. Inst. Invest. Geol. «Lucas Mallada»*, Madrid, 16: 205-242.

Vergés J. y Muñoz J.A. (1990): Thrust sequences in the southern central Pyrenees. *Bulletin Societé Géologique de France*, 8 6(2): 265-271.

Wilkerson, M. S., Apotria, T. y Farid, T. (2002): Interpreting the geologic map expression of contractional faiult-related folds terminations: lateral/oblique ramps vesus displacement gradients. *Journal of Structural Geology*, 24: 593-607.

Manuscrito recibido el 28 de mayo de 2007
Aceptado el manuscrito revisado el 27 de agosto de 2007

Sites	D&I	α 95	k	β	Number of specimens	Age	References
74. Aísa R. Aragón	16 , 42	9	30	+11	77	Upper Cretaceous	Oliva and Pueyo, 2007
75. S. Bernera	21 , 47	5	75	+16	101	Upper Cretaceous	Oliva and Pueyo, 2007
73. Collarada-Partacua	21 , 52	9	26	+26	73	Upper Cretaceous	Oliva and Pueyo, 2007
72. Flysch	27 , 34	5	46	+22	38	Eocene	Oliva and Pueyo, 2007
71. Tendenera-Otal	31 , 31	9	34	+26	73	Upper Cretaceous	Oliva and Pueyo, 2007
69. Tourrettes-Añisclo	350 , 45	13	18	+11	12	Upper Cretaceous	Oliva and Pueyo, 2007
68. Bielsa	6 , 36	5	46	+1	150	Triassic	Oliva , 2004
50. 90J-32+33+34+35	38 , 28	11	55	+33	14	Ypresiense	Dinarès, 1992
9. Yesa	54 , 51	13	19	+16	57	Eocene	Pueyo, 2000
14. Bagüés	17 , 18	13	5	+12	33	Upper Eoc.-Oligoc.	Hogan, 1993
16. Sta. Bárbara (N)	21 , 34	10	14	+16	17	Upper Eoc.-Oligoc.	Pueyo, 2000
15. Alastruey	41 , 28	18	11	+22	24	Bartonian	Hogan, 1993
15	193 -22	20	9				
25. Jaca-Bal Estrecha	11 , 52	15	22	+6	43	Bartonian-Priabonian	Pueyo, 2000
26. Oroel N.	30 , 57	16	11	+25	8	Bartonian-Priabonian	Pueyo, 2000
38. Monrepós N.	9 , 43	7	26	+4	18	Bartonian-Priabonian	Pueyo, 2000
77. R- Gállego	17 , 47	9	8	+12	36	Middle Eocene	Oms et al., 2003
39. Basa	25 , 36	6	3	+30	39	Bartonian	Pueyo, 2000
40. Yebra de Basa	11 , 38	9	68	+25	66	Bartonian	Hogan, 1993
40	228 , -45	31	3				
41. Guarguera N	37 , 39	7	17	-32	27	Upp. Eoc.- Oligocene	Pueyo, 2000
44. Jánovas	42 , 38	15	6	+37	20	Bartonian-Priabonian	Pueyo, 2000
64. YB+BB+90J39	61 , 43	12	68	+57	19	Ilerd.-Ypresian	Dinarès 1992, Fernández 2004
62. CB+SB+GB	69 , 54	13	59	+64	23	Lower Lutetian	Fernández, 2004
63. 90J38+25	43 , 25	4	2383	+37	6	Lutetian	Dinarès, 1992
61. EML+PML+SML	34 , 45	17	37	+29	20	Middle-Upp. Lutetian	Fernández, 2004
48. Mediano	22 , 53	6	14	+22	92	Upp. Eoc.- Oligocene	Bentham, 1992
48	212 , -25	15	9				
12. S Marzal N.	30 , 55	20	9	+25	6	Bartonian	Pueyo, 2000
18. Sto. Domingo N.	47 , 40	10	14	+42	16	Bartonian	Pueyo, 2000
19.Riglos	7 , 30	19	19	+2	58	Bartonian-Priabonian	Pueyo, 2000
23. Sta. Bárbara S.	34 , 44	16	9	+29	11	Bartonian-Priabonian	Pueyo, 2000
22. S. Salinas	22 , 37	15	17	+17	66	Bartonian	Pueyo, 2000
30. Oroel S.	23 , 49	19	7	+18	10	Bartonian-Priabonian	Pueyo, 2000
32. S. Caballera	29 , 45	12	35	+24	45	Bartonian	Pueyo, 2000
33. S. Gratal	26 , 48	12	78	+21	31	Bartonian	Pueyo, 2000
34. Arguis	10 , 35	9	7	+12	63	Bartonian	Hogan, 1993
34	203 , -43	29	4				
35. S. Águila	22 , 51	10	61	+17	42	Bartonian	Pueyo, 2000
43. S. Guara	21 , 41	11	18	+16	100	Bartonian	Pueyo, 2000
45. Almanzore	2 , 48	25	8	+15	18	Bartonian	Bentham, 1992
45	218 , -24	32	8				
46. Eripol	34 , 54	8	12	+14	63	Upp- Eocene- Oligocene	Bentham, 1992
46	184 , -20	21	6				
47. Ligüerre	12 , 51	12	9	+16	58	Middle-Upp. Eocene	Bentham, 1992
47.	209 , -54	15	8				

Annex.- Same legend as in table I